

Effect of Nano-SiC Particles on Properties of the Ni-SiC Gradient Composite Coating

Liqin Shen

School of Rail Transportation, Nanjing Vocational Institute of Transport Technology, Nanjing, China

Abstract:

In this paper, Ni based gradient composite coatings containing micro- and nano-SiC particles was prepared by dipulse electrodeposition in watts nickel solution. The effect of nano-SiC added in the solution on the micro morphology, wear-and corrosion resistance of the coating was investigated. The results show that the grain size of Ni-SiC gradient composite coatings is fined when adding nano-SiC in electrolyte; the maximum microhardness of gradient coating is 553 HV, and the average coefficient of gradient coating with 0.41 are about 1.5 times and 4/5 than that of micro-SiC gradient composite coating; and shows the best corrosion resistance which the values of corrosion current density with $1.957 \times 10^{-7} \text{A.cm}^2$ is about 1/10 than that of micro-SiC gradient composite coating.

Keywords: Ni-SiC gradient composite coating, Nano-SiC, Wear resistance, Corrosion resistance.

I. INTRODUCTION

Owing to low density, good ductility and toughness, and easy machining, aluminum and aluminum alloys have been widely used in various industrial sectors. In practical applications, however, disadvantages such as low hardness, poor wear resistance and frequent abrasion have limited the wider application of aluminum alloy materials. Currently, major surface treatment methods used to improve the aluminum alloy properties include the micro-arc oxidation [1-3], laser treatment [4, 5], electroless plating [6, 7], electroplating [8, 9] and anodization [10, 11]. Through these surface treatment techniques, the corrosion and wear resistances of aluminum alloys have been greatly improved.

Ni-SiC composite coatings have the advantages of high hardness and good wear, oxidation and corrosion resistances, which are widely used in internal combustion engines, die-casting molds and engine cylinders [12]. Although extensive research has been conducted on nano-Ni-SiC composite and gradient coatings at home and abroad [13-17], the majority of them

focus on the effects of process parameters on the coating microhardness, composition and corrosion resistance, while the effect of nanoparticles on the properties of micro-gradient coatings has scarcely been reported. To this end, we fabricated Ni-SiC gradient composite coating containing nano-SiC on the surface of LY12 aluminum alloy by dipulse electrodeposition, and investigated the effects of nano-SiC particles in the electrodepositing solution on the wear and corrosion resistances of the fabricated coating.

II. EXPERIMENTAL

Using pure nickel plate as anode, and LY12 aluminum alloy sample (15× 15× 3.0mm) as cathode, the Ni-SiC gradient composite coating was deposited on the surface of aluminum alloy by using dipulse electrodeposition power supply (SMD-30P). Table I details the composition of electrodepositing solution and the electrodeposition conditions.

TABLE I. The electrodeposition parameters for Ni/SiC composite coatings

SOLUTION COMPOSITION (G.L-1)		ELECTRODEPOSITION CONDITIONS	
NISO ₄ .6H ₂ O	300	pH	4.5~5.5
NICL.6H ₂ O	30	Temperature	30±1°C
H ₃ BO ₃	35	Stirring rate	250 rpm
SIC POWDER(5MM))	20,40,60,80,100	Current density	2.5 A.dm ⁻²
SIC POWDER(40NM)	2.0	Duty cycle(d.c)	50%
		Time (h)	5
		Pulse frequency(v)	1000Hz

Generally, when nano-SiC particles are added to the electrodepositing solution at room temperature, they always float on the solution surface and require prolonged stirring to enter the solution, thus resulting in long pretreatment time. Prior to electrodeposition, preweighed nano-SiC particles were added with an appropriate amount of electrodepositing solution and heated using a water bath. Meanwhile, surfactant was added dropwise, so that the nano-SiC particles were quickly wetted by the electrodepositing solution to enter it. Next, some of the electrodepositing solution containing wetted nano-SiC particles was added into the electroplating beaker, stirred at 800rpm and ultrasonicated for 15min. Afterwards, 20g/L micro-SiC particles were added at 1-h intervals to perform composite electrodeposition, thereby fabricating the nano-SiC-containing Ni-SiC gradient composite coating.

Utilizing FM700 microhardness tester, the microhardness of the gradient composite coating was measured at an indenter load of 100g and a loading time of 15s. Five values were

measured at different sites of coating cross section, and then averaged.

Friction experiment of the gradient composite coating was conducted with MFT-3000 tribometer (RTEC) under the following conditions: GCr15 ball (ϕ 10mm, quenched, hardness: HRC63) friction material, reciprocation speed 10m/s, dry grinding, radius 2mm, load 16N, room temperature, and time 30min.

Electrochemical test was completed on the PARSTAT 2273 workstation. A three-electrode system was adopted, where the auxiliary electrode was a platinum electrode, the reference electrode was a saturated calomel electrode (SCE), and the working electrode was the sample. A 3.5% NaCl aqueous solution was used as the test solution, and the pretest stabilization time was set at 60 min. In the Tafel extrapolation test, the scan range was the self-corrosion potential ($E_{\text{corr}} \pm 1.5$) V, and the scan rate was 5mV/min.

JSM-6380LV SEM equipped with EDS was utilized to analyze the microstructures of gradient composite coating and wear track surfaces. The composite coating structure was analyzed via Bruker D8 Advance rotating target XRD under the following conditions: Cu rotating target, Cu-K α excitation, tube current 40 mA, tube voltage 40 kV, step size 0.02°, and scanning rate 5.0°/min.

III. RESULTS AND DISCUSSION

3.1 Effect of Nano-SiC on the Coating Microstructure

Fig. 1 illustrates the microstructures of the Ni-SiC gradient coatings, where no nano-SiC particles were added into the electrodepositing solution in Fig. 1(a), and 2.0 g/L nano-SiC particles were added into the solution in Fig. 1(b). As is clear, the addition of nano-SiC particles had a prominent effect on the microstructure of the composite coating. According to Fig. 1(a), when no nano-SiC particles were added into the electrodepositing solution, random distribution of micro-sized SiC particles was observable on the Ni-SiC composite coating surface. Meanwhile, presence of cavities was noted, which were left by the scoured SiC particles not firmly wrapped by matrix metal, and the coating surface was incompact. According to Fig. 1(b), after adding 2.0g/L nano-SiC particles into the electrodepositing solution, the coating surface was cystiform, which was constituted by smaller crystal grains that were obviously refined. Meanwhile, the compactness of the composite coating was slightly improved. The reason was that appropriate addition of nano-SiC into the electrodepositing solution provided more activation sites during the deposition of matrix metal, which led to increased nucleation sites of Ni metal, thereby refining the crystal grains.

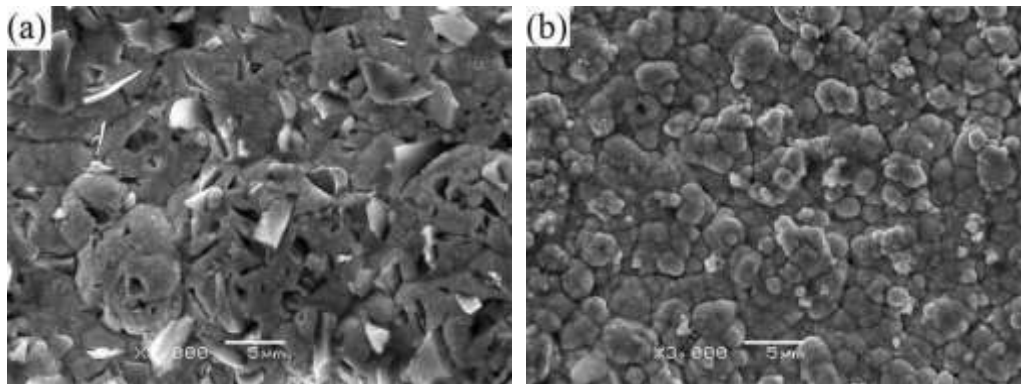


Fig.1: SEM images of the surface of gradient composite coatings: (a) without nano-SiC; (b) with nano-SiC 2.0g/L

3.2 Effect of Nano-SiC on the Coating Texture

Fig. 2 displays the XRD patterns of coatings, where Fig. 2(a) shows the spectra of pure Ni coating and Figs. 2(b) and (c) show the spectra of gradient coatings without or with nano-SiC particles. As is clear, all the gradient coatings were composed of matrix phase Ni and SiC phase. After adding SiC particles into the electrodepositing solution, the Ni in the coating preferentially grew on the (200) crystal plane and transformed into the (111) plane. This was probably attributed to the coexistence of micro- and nano-SiC particles in the electrodepositing solution, which led to change in the preferentially oriented plane of Ni during the electrocrystallization process.

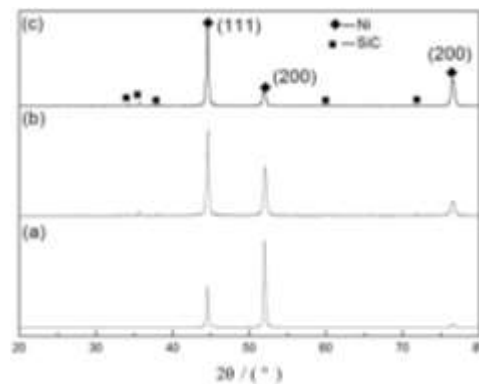


Fig.2: XRD patterns of coatings: (a) nickel coating; (b) Ni-SiC composite; (c) Ni-SiC composite with nano-SiC

Fig. 3 illustrates the cross-sectional microstructures of the Ni-SiC gradient coatings. Uniform gradient dispersion of SiC particles were observed in the coatings, and the coating particle content increased with the furthering distance from the interface. The reason was that under fixed stirring rate of electrodepositing solution and cathode current density, the amount of SiC particles deposited in the coatings increased with the rise in their addition into the solution.

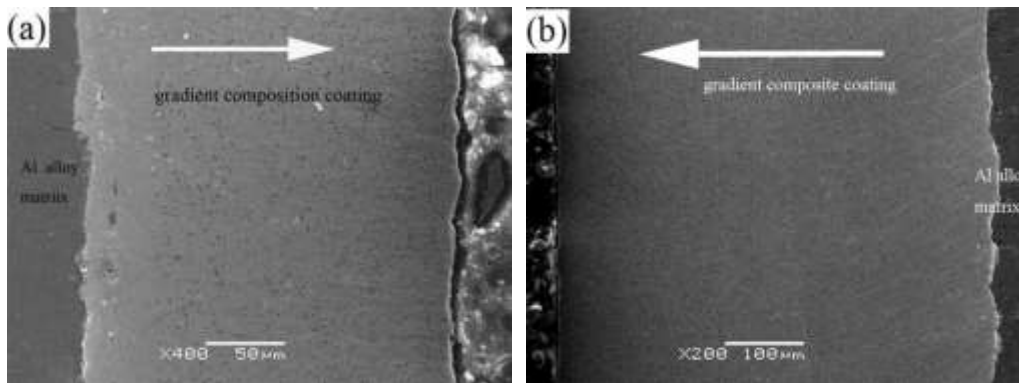


Fig. 3: SEM images of the cross-section of Ni-SiC composite coatings: (a) without nano-SiC; (b) with nano-SiC

3.3 Effect of Nano-SiC on the Coating Tribological Properties

Fig. 4 plots the microhardness (a) and friction coefficient (b) variations of the gradient coatings. According to Fig. 4(a), all the microhardness values exhibited gradient increases with the furthering distance from the matrix/coating interface, peaking at the outer coating rims. The maximum microhardness was 367HV when only micro-SiC was added into the electrodepositing solution, and was 553HV when both micro- and nano-SiC particles were added, showing 5.6- and 3.6-folds greater values than that of the pure Ni coating, respectively. This was attributed to the role of micro-SiC in holistically strengthening the composite coating. Contrastively, after adding nano-SiC particles into the electrodepositing solution, they were co-deposited with micro-SiC particles to locally strengthen the matrix around the micro-SiC particles. The integration of holistic and local effects enhanced the plastic deformation resistance of the nano-SiC-containing coating, which thus exhibited higher microhardness.

Fig. 4(b) depicts the temporal variations of the coating friction coefficients. As is clear, the friction coefficient of pure Ni coating fluctuated drastically within the sliding time, with an average of approximately 0.56. Contrastively, the friction coefficient of Ni-SiC gradient coatings decreased slightly, which fluctuated little during the sliding time, basically maintaining at 0.45. The gradient coating containing nano-SiC particles showed the smallest friction coefficient. With the prolongation of sliding time, the friction coefficient tended to decrease slowly, reaching a minimum of 0.36. Based on a combination of Figs. 4(a) and (b), a certain correspondence existed between the coating microhardness and the friction coefficient. The composite coating with higher microhardness had lower friction coefficient.

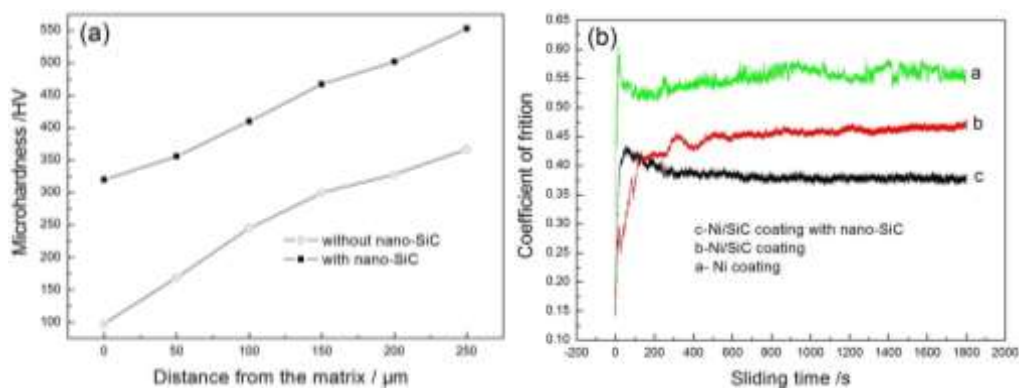


Fig. 4: Relationship between coefficient and time: (a) nickel; (b) Ni-SiC composite; (c) Ni-SiC composite with nano-SiC

Fig. 5 illustrates the micromorphology of wear tracks on the gradient coating surfaces. Clearly, material transfer and shallow furrowing were present on all the wear track surfaces of composite coating, indicating a mixed mechanism of abrasive-adhesive wear. As shown in Fig. 5(a), the coating without nano-SiC addition had shallow furrows on the wear track surface. Meanwhile, substantial cavities were observed on the wear track surface as well. Some of the cavities were leftovers from the original coating surface, while the remaining was left by the detachment of SiC particles from the matrix metal during the friction process. As shown in Fig. 5(b), after adding nano-SiC particles into the electrodepositing solution, the wear tracks of the coating were tire-patterned and tightly arranged, with distribution of small aperture cavities on the surface. The wear failure of gradient coatings was attributed primarily to the filling of cavities by the wear debris resulting from hard particle extrusion and ploughing, or the entrapment of the wear debris between wear surfaces, which acted as new abrasive particles. Additionally, the low-hardness matrix metal Ni underwent obvious plastic deformation, extrusion and detachment during friction with the high-hardness grinding ball. For the

nanoparticle-containing gradient coating, the microparticles in the coating served as hard particles, and the grinding ball was shallowly pressed into the coating surface, which led to reduced contact area between friction pair and coating, thus forming a shallow furrowed wear track morphology. Meanwhile, the nanoparticles were deposited in the Ni layer between microparticle gaps, locally strengthening the Ni coating around the micro-SiC particles, and enhancing the microparticle holding force of the Ni coating. As a result, the detachment probability of the hard micro-SiC particles was greatly reduced during the wear process. In summary, at concentrations where the addition of nano-SiC particles into the micro-SiC-containing electrodeposition solution did not cause the nanoparticle aggregation, the nano-SiC particles were evenly dispersed in the solution, which were co-deposited with the micro-SiC particles during the electrodeposition process, thereby achieving the holistic and local strengthening of matrix metal, and enhancing the composite coating properties.

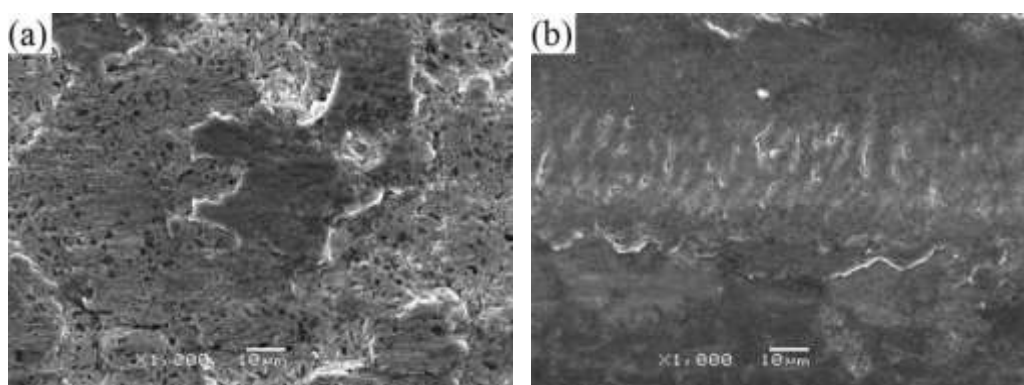


Fig. 5: SEM morphology of the wear tracks of the composites coatings: (a) Ni-SiC composite; (b) Ni-SiC composite with nano-SiC

3.4 Effect of nano-SiC on the Coating Corrosion Resistance

Fig. 6 displays the Tafel curves of pure Ni coating, Ni-SiC coating and nano-SiC-containing Ni-SiC coating. It is clear that compared to the pure Ni coating, the two Ni-SiC gradient coatings both exhibited better corrosion resistance, especially the one containing nano-SiC. The SiC particles and Ni were co-deposited to form a composite coating, thereby increasing the self-corrosion potential from -0.50 V (pure Ni coating) to -0.36V and decreasing the density of self-corrosion current from $4.977 \times 10^{-6} \text{ A/cm}^2$ to $1.665 \times 10^{-6} \text{ A/cm}^2$. After adding nano-SiC particles into the electrodeposition solution, the self-corrosion potential and current density of the gradient coating were -0.36V and $1.957 \times 10^{-7} \text{ A/cm}^2$, respectively. Thus, clearly, the major determinants of electrochemical corrosion resistance were the base

metal potential and the coating compactness. Due to the integration of SiC, the matrix metal led to increased potential. Meanwhile, the co-deposition of micro- and nano-SiC played a role in achieving effective coating densification, so that the Cl⁻ in the corrosive electrolyte could not easily penetrate through the compact coating. Additionally, the micro- and nano-SiC particles in the coating also facilitated the blockage of Cl⁻ penetration, thereby improving the composite coating resistance to electrochemical corrosion.

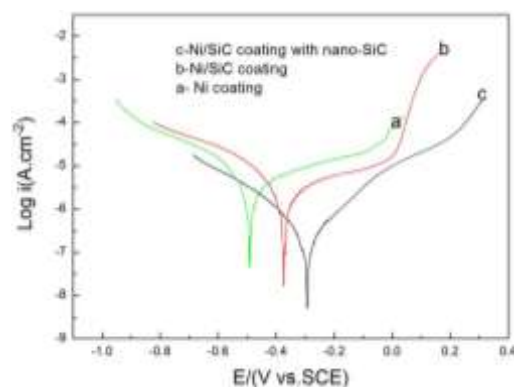


Fig. 6: Tafel curves of coatings

IV. CONCLUSION

1) By adjusting the electrodeposition solution concentration of SiC particles, the Ni-SiC composite coatings are fabricated on the aluminum alloy surface, where the SiC particles show a gradient distribution. After adding nano-SiC particles, the crystal grains of Ni coating are refined. However, the microstructures of the gradient coatings are not obviously affected, all of which are in the Ni+SiC phase.

2) Compared to the micro SiC-reinforced gradient coating, after adding nano-SiC particles into the electrodeposition solution, the coating microhardness increases to 553HV, which is 1.5 and 5.6 times that of the micro-composite coating and pure Ni coating, respectively. Besides, the nano-SiC-containing coating exhibits a friction coefficient of 0.36, which is 4/5 and 3/5 that of the micro-composite and pure Ni coatings, respectively. Further, its corrosion current density is 1.957×10^{-7} A/cm², which is 1/10 that of the micro-composite coating and 1/25 that of the pure Ni coating.

ACKNOWLEDGEMENTS

This research was supported by High Research Project for Teacher Professional Leaders of Higher Vocational Colleges in Jiangsu (Grant No. 2020GRFX055) and Higher Vocational Education Research Fund Project in Nanjing Vocational Institute of Transport Technology (Grant No.19JY003) and Transportation Vocational Education and Scientific Research Project in the National Transportation Vocational Education and Teaching Steering Committee (Grant No. 2019A02)

REFERENCES

- [1] Wang P, Li JP, Guo YC, Wang JL, Yang Z, Liang MX (2016) The formation mechanism of the composited ceramic coating with thermal protection feature on an Al₂Si piston alloy via a modified PEO process. *Journal of Alloy and compounds* 82: 48–55
- [2] Xiang N, Song RG, Zhao J, Li H, Wang C, Wang ZX (2015) Microstructure and mechanical properties of ceramic coatings formed on 6063 aluminium alloy by micro-arc oxidation. *Transactions of Nonferrous Metals Society of China* 25(10): 3323–3328
- [3] Li YD, Zhang Y, Li SM, Zhao PZ (2016) Influence of adipic acid on anodic film formation and corrosion resistance of 2024 aluminum alloy. *Transactions of Nonferrous Metals Society of China* 26(2): 492–500
- [4] Ravi SR, Hitesh D, Vora SG, Srinivasan N, Dahotre B (2015) Laser alloyed Al-W coatings on aluminum for enhanced corrosion resistance. *Applied Surface Science* 328: 205–214
- [5] Leo N-Patinon CA, Aguilar-Reyes EA, Bedolla-Becerril E, Bedolla-Jacuinde A, Me Ndez-Diaz S (2013) Dry sliding wear of gradient Al-Ni/SiC composites. *Wear* 301: 688–694
- [6] Amatoc D, Buhagiar J, Betts JC (2014) Tribological characteristics of an A356 aluminium alloy laser surface alloyed with nickel and Ni-Ti-C. *Applied Surface Science* 313: 720–729
- [7] Sribalajia M, Arunkumar P, Suresh Babub K, Anup Kumar K (2015) Crystallization mechanism and corrosion property of electroless nickel phosphorus coating during intermediate temperature oxidation. *Applied Surface Science* 355: 112–120
- [8] Li B, Chen Y, Huang W, Yang WZ, Yin XS, Liu Y (2016) Enhanced corrosion resistance of hydroxyapatite/magnesium-phosphate-composite-coated AZ31 alloy co-deposited by electrodeposition method. *Ceramics International* 42: 13074–13085
- [9] Florent C, Pierre-Louis T, Laurent A (2016) Innovating pulsed electrophoretic deposition of boehmite nanoparticles dispersed in an aqueous solution, into a model porous anodic film, prepared on aluminium alloy 1050. *Surface & Coatings Technology* 302: 293–301
- [10] Kong De Jun, Wang Jin Chun. (2015) Salt spray corrosion and electrochemical corrosion properties of anodic oxide film on 7475 aluminum alloy. *Journal of Alloys and Compounds* 632: 286–290
- [11] Maximilian S, Ingolf S, Franziska H, Anja S, Dagmar B, Sebastian B, Eckhard B, Uwe G, Thomas L (2016) Anodic oxidation of AlMgSi₁-Coatings' mechanical properties, process costs and energy consumption of the oxide formation. *Materials and Design* 89: 1259–1269

- [12] Gyftou P, Pavlatou E A, Spyrellis N (2008) Effect of pulse electrodeposition parameters on the properties of Ni/nano-SiC Composites. *Applied Surface Science* 254 (18): 5910–5916
- [13] Wang Y, Yuan XT, Sun DB, Yu HY (2012) Electrochemical Behavior and Corrosion Resistance of Electroplated Nickel - Phosphorus /Nanometer Silicon Carbide Composite Coating. *Journal of Materials Protection* 45(5): 1–5
- [14] Ma CY, Ding JJ, Chu DQ (2012) Effect of pulse electrodeposition parameters on the performance of Ni-SiC composite coatings. *Ordnance Material Science and Engineering* 35(4): 65–67
- [15] Yang XX, Zhang M, Huang Y, Hu XG, Pan YL, Cheng SH, Du M, Ding YW (2014) Preparation and friction and wear resistance of SiC/Ni Nano-composite coatings. *Material for Mechanical Engineering* 38(7): 53–57
- [16] Wang L, Sun BL, Xu W, Jiang XM, Zhang L, Lin HL (2012) Influences of technological parameters on the hardness of Ni-SiC Nano-composite. *Plating and Finishing* 34(5): 8–11
- [17] Lari Baghal SM, Heydarzadeh Sohi M, Amadeh A (2012) A functionally gradient nano-Ni-Co/SiC composite coating on aluminum and its tribological properties. *Surface & Coatings Technology* 206 (19/20): 4032–4039